A Voltage-Based Fault Location Algorithm for Medium Voltage Active Distribution Systems

C. G. Arsoniadis, C. A. Apostolopoulos, P. S. Georgilakis, V. C. Nikolaidis*

***Abstract*--This paper addresses a fault location algorithm appropriate for unbalanced medium voltage overhead distribution systems with or without distributed generation. The proposed algorithm utilizes only synchronized voltage measurements from two measurement points inside the distribution system. The algorithm accurately estimates the fault position for any type of short-circuit faults by applying fundamental bus-impedance-matrix-based fault analysis. Fault resistance is considered in the algorithm but not explicitly included in the bus impedance matrix. Simulation results show a good performance of the fault location algorithm under various pre-fault operation conditions of a test distribution system.**

***Keywords*: active distribution systems, distributed generation, fault location, synchronized measurements.**

I. Introduction

DUE to their nature, length and operation conditions, overhead distribution lines are more frequently exposed to short-circuit faults stemming from various causes (e.g. lightning, adverse weather conditions, trees, animals, etc.). Protection means must quickly isolate the faulted line segment in order to minimize its damage and the impact of the fault on the rest of the system. At the same time, fault locators (FLs) may be assigned to locate the exact fault position. Prompt and accurate estimation of the fault position reduces the restoration time, time of interruption supply, and generally improves the reliability of the system [1].

Most fault location methods for power distribution systems utilize fundamental-frequency voltage and/or current measurements together with the passive network parameters to implement a fault location algorithm. Since installing voltage/current measuring devices (MDs) at every system bus is not economically feasible, a few MDs are used instead. In [2], pre- and during-fault voltage and current phasors taken from the root node, as well as voltage sag magnitudes taken from some nodes along the feeder, are utilized to match these actual measurements with the solution of a backward/forward sweep during-fault power flow method. A promising two-step fault location procedure based on voltage and current measurements taken from two measurement points inside the distribution system is addressed in [3]. A systematic fault location procedure based on voltage and current measurements that are taken from a single point, which is the feeder departure at the main high voltage/medium voltage (HV/MV) substation, and on the use of the system bus impedance matrix, is presented in [4].

A few fault location methods are solely based on voltage measurements. In this category, [5] and [6] give satisfactory fault location estimations and additionally emphasize in reducing the required number of measurement points. The method proposed in [7] uses negative-sequence voltage amplitudes calculated from sparse measurements along the distribution feeder to locate the faulted section. Although this method does not exactly use voltage phasors, it is fundamentally based on the classic circuit theory, whereas a more sophisticated sub-algorithm minimizes the required measurement points. A recently proposed method [8] requires two synchronized and few non-synchronized pre- and during-fault voltages at few buses along with the impedance matrix to estimate the fault position.

The fault location methods presented in [6], [9]-[12] utilize measurements from a few buses to estimate the fault location in distribution systems but do not consider distributed generation (DG). Other techniques [5], [8], [13] consider DG but use synchronized/unsynchronized voltage measurements from more than two buses. In [2], [9], [11] the fault position is found based on the best match between calculated and measured voltage sags. In those works, the fault current is estimated at first and then it is injected to each analyzed node of the distribution system under investigation. The voltage variations caused by the fault current injection, are compared with the measured voltage sags and the best match indicates the actual fault node. In [5] and [7], the sparse matrix representation approach is adopted. Because of the use of a limited number of phasor measurement units (PMUs), the set of equations derived from the aforementioned matrix approach is underdetermined. This problem is handled in [5] through comprehensive sensing. The Bayesian comprehensive sensing method is utilized in [7] for the same purpose.

In general, all the above-mentioned research works provide good fault location results under specific conditions

European Union
European Social Fund

Operational Programme
Human Resources Development, Education and Lifelong Learning
Co-financed by Greece and the European Union

ΕΣΠΑ 2014-2020

This research is co-financed by Greece and the European Union (European Social Fund- ESF) through the Operational Programme «Human Resources Development, Education and Lifelong Learning 2014-2020» in the context of the project "Automated fault location in active distribution systems using a novel fault location algorithm and fault passage indicators" (MIS 5049903).

V. C. Nikolaidis and C. G. Arsoniadis are with the Department of Electrical and Computer Engineering, Democritus University of Thrace, Xanthi 67100, Greece (e-mails: *vnikolai@ee.duth.gr; carsonia@ee.duth.gr).
C. A. Apostolopoulos is with Ariadne Interconnection S.P.L.C, 12132 Athens, Greece (email: capostolopoulos81@gmail.com).
P. S. Georgilakis is with the School of Electrical and Computer Engineering, National Technical University of Athens (NTUA), 9 Heroon Politechniou street, Athens, Greece (e-mail: pgeorg@power.ece.ntua.gr).

Paper submitted to the International Conference on Power Systems Transients (IPST2021) in Belo Horizonte, Brazil June 6-10, 2021.

concerning distribution network configuration, fault type, DG technology, data type (synchronized or not) and availability, and measurement errors. In this sense, each of the methods of the bibliography has weak points, which is absolutely normal when dealing with such a complex research problem. Review paper [14] provides a thorough insight on the principles of most of the abovementioned fault location methods, whereas a more recent review paper [15] gives the trends for fault location in complex distribution systems (i.e., microgrids).

This paper delivers detailed results of an extended evaluation of a new fault location method for medium voltage overhead distribution systems. The fault location algorithm is based on fundamental short-circuit fault analysis utilizing recorded three-phase voltage signals from two measurement points, as well as the network bus impedance matrix $\mathbf{Z}_{\mathbf{bus}}$. The latter is pre-calculated for each possible network topology and stored in the fault locator's database. Simulation results of the fault location algorithm proposed in this paper show that it has sufficient accuracy, although only synchronized voltage measurements from two points of the distribution network are taken. In addition, the algorithm is adequate irrespective if DG is present or not in the distribution system.

Comparing with other papers in the literature and especially with [4], the following differences/advantages arise:

- The mathematical formulation of our method makes it directly applicable for effectively locating faults in single-source and multi-source distribution systems, as does also the method of [4].
- Only voltage measurements from two arbitrary points inside the distribution system of interest are required in our method. Current measurements are not at all needed. Subsequently, current transformer (CT) saturation effect and other related problems do not affect our method. On the contrary, the method presented in [4] is based on voltage and current measurements. In the multi-source algorithm of [4], pre-fault currents are utilized; hence CT saturation is not a problem. However, in the single-source algorithm of [4], during-fault currents are utilized. Thus, CT saturation may affect the fault location results.
- The fault location method proposed in our paper does not require the construction of the complete bus impedance matrix $\mathbf{Z}_{\mathbf{bus}}$, meaning that fault resistance is not included in $\mathbf{Z}_{\mathbf{bus}}$. Reference [4] explicitly considers fault resistance. In other words, the mathematical formulation of our method is simpler than that of [4].
- Overall, the fault location estimation results of our method are comparable with that of other efficient methods in the literature including [4].

The structure of the paper is as follows. Section II includes the formulation steps of the fault location algorithm for single-phase and three-phase distribution systems. Section III presents the simulation results evaluating algorithm's performance. Section IV summarizes the main findings and concludes the paper.

II. Proposed Fault Location Algorithm

The proposed fault location method will be explained with the aid of the simple, generic, three-phase distribution system depicted in Fig. 1. In general, this system comprises of three-phase, two-phase, or single-phase line sections and loads. However, to better understand the main idea of the fault location method, the distribution system of Fig. 1 is initially assumed single-phase. The extension of the method for unbalanced three-phase distribution systems will follow.

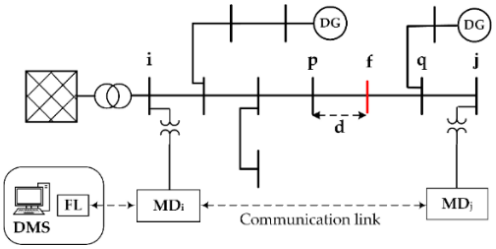

Fig. 1. Simple radial power distribution system.

A. Algorithm Formulation for Single-Phase Circuits

Consider a short-circuit fault occurring within the line segment linking buses p and q. The goal of the fault location method is to accurately estimate the distance d of the fault position from the preceding bus p. By utilizing the voltage drop due to the steady-state short-circuit fault, measured at two particular points, i.e. at the substation bus i and at any other arbitrary bus j, an analytical expression of the desired distance d can be derived. This is realized if the measured voltage drops ΔV_i and ΔV_j are expressed as a function of the steady-state fault current injected into the (fictitious) faulted bus f and the respective transfer impedance:

$$\Delta V_i = -Z_{if} I_f \tag{1}$$

$$\Delta V_j = -Z_{jf} I_f \tag{2}$$

where ΔV_i, ΔV_j is the voltage drop due to the short-circuit fault at bus i and j, respectively, I_f is the steady-state short-circuit current flowing from the fault position to the reference bus, and Z_{if}, Z_{jf} is the transfer impedance between bus i and bus f and between bus j and bus f, respectively.

The voltage drops are defined as below:

$$\Delta V_i = V_i^f - V_i^{pf} \tag{3}$$

$$\Delta V_j = V_j^f - V_j^{pf} \tag{4}$$

where the superscript pf and f corresponds to the pre-fault and during-fault voltage phasor of bus i and j, respectively.

The short-circuit fault current I_{sc} can be eliminated after proper manipulation of (1) and (2):

$$\frac{\Delta V_i}{\Delta V_j} = \frac{Z_{if}}{Z_{jf}} = \gamma \tag{5}$$

The transfer impedance between any arbitrary bus n and the faulted bus f can be expressed as follows [4]:

$$Z_{nf} = Z_{np} - d(Z_{np} - Z_{nq}) \tag{6}$$

where Z_{np} is the transfer impedance between bus n and bus p, Z_{nq} is the transfer impedance between bus n and bus q, and d is the fault distance from the preceding bus p.

By combining (5) and (6), the fault distance d can be estimated from (7), which is a function of the transfer impedances between the end-buses of a particular line section and the measured buses:

$$d = \frac{Z_{ip} - \gamma Z_{jp}}{(Z_{ip} - \gamma Z_{jp}) - (Z_{iq} - \gamma Z_{jq})} \tag{7}$$

In fact, this method successively applies (7) for each particular feeder line segment after a fault is identified. Hence, multiple normal solutions (i.e. $d \in [0,1]$ p.u.) may be found.

Note also that the driving point and transfer impedances required in the fault location algorithm are derived from the bus impedance matrix $\mathbf{Z}_{\mathbf{bus}}$, previously constructed for the system under examination. The latter assumes that the exact distribution system topology remains unchanged and that it is already known to the distribution system operator.

B. Algorithm Formulation for Unbalanced Three-Phase Circuits

1) Basic Formulation

In the previous subsection, the analysis concerned single-phase circuits, where each bus corresponds to a single node of the circuit. In the general three-phase circuit representation, each bus corresponds to up to three nodes. Hence, a three-phase line segment linking buses p and q is represented as in Fig. 2. In this figure, bus f is again the faulted bus.

Now, (1) and (2) take the matrix form of (8) and (9), respectively:

$$\begin{bmatrix} \Delta V_{i,a} \\ \Delta V_{i,b} \\ \Delta V_{i,c} \end{bmatrix} = - \begin{bmatrix} Z_{i_a f_a} & Z_{i_a f_b} & Z_{i_a f_c} \\ Z_{i_b f_a} & Z_{i_b f_b} & Z_{i_b f_c} \\ Z_{i_c f_a} & Z_{i_c f_b} & Z_{i_c f_c} \end{bmatrix} \begin{bmatrix} I_{f,a} \\ I_{f,b} \\ I_{f,c} \end{bmatrix} \tag{8}$$

$$\begin{bmatrix} \Delta V_{j,a} \\ \Delta V_{j,b} \\ \Delta V_{j,c} \end{bmatrix} = - \begin{bmatrix} Z_{j_a f_a} & Z_{j_a f_b} & Z_{j_a f_c} \\ Z_{j_b f_a} & Z_{j_b f_b} & Z_{j_b f_c} \\ Z_{j_c f_a} & Z_{j_c f_b} & Z_{j_c f_c} \end{bmatrix} \begin{bmatrix} I_{f,a} \\ I_{f,b} \\ I_{f,c} \end{bmatrix} \tag{9}$$

where subscript a, b, and c indicates the corresponding phase.

The expansion of (8) and (9) is as follows:

$$\Delta V_{i,a} = -Z_{i_a f_a} I_{f,a} - Z_{i_a f_b} I_{f,b} - Z_{i_a f_c} I_{f,c} \tag{10}$$

$$\Delta V_{i,b} = -Z_{i_b f_a} I_{f,a} - Z_{i_b f_b} I_{f,b} - Z_{i_b f_c} I_{f,c} \tag{11}$$

$$\Delta V_{i,c} = -Z_{i_c f_a} I_{f,a} - Z_{i_c f_b} I_{f,b} - Z_{i_c f_c} I_{f,c} \tag{12}$$

$$\Delta V_{j,a} = -Z_{j_a f_a} I_{f,a} - Z_{j_a f_b} I_{f,b} - Z_{j_a f_c} I_{f,c} \tag{13}$$

$$\Delta V_{j,b} = -Z_{j_b f_a} I_{f,a} - Z_{j_b f_b} I_{f,b} - Z_{j_b f_c} I_{f,c} \tag{14}$$

$$\Delta V_{j,c} = -Z_{j_c f_a} I_{f,a} - Z_{j_c f_b} I_{f,b} - Z_{j_c f_c} I_{f,c} \tag{15}$$

The boundary conditions for the most common short-circuit fault types are given below:

$$I_{f,a} \neq 0, \quad I_{f,b} = I_{f,c} = 0 \quad (ag\ fault) \tag{16}$$

$$I_{f,c} = 0, \quad I_{f,a} + I_{f,b} = 0 \quad (ab\ fault) \tag{17}$$

$$I_{f,c} = 0, \quad I_{f,a} + I_{f,b} = I_{f,g} \quad (abg\ fault) \tag{18}$$

$$I_{f,a} + I_{f,b} + I_{f,c} = 0 \quad (abc\ fault) \tag{19}$$

2) Analysis for Single-Line-Ground Short-Circuit Faults

For the case of a phase-a-to-ground (ag) fault, the boundary conditions are expressed by (16). Hence, (10)–(15) take the following compact form:

$$\Delta V_{i,k} = -Z_{i_k f_a} I_{f,a} \tag{20}$$

$$\Delta V_{j,k} = -Z_{j_k f_a} I_{f,a} \tag{21}$$

where $k = a, b, c$.

After mathematical manipulations between the six equations of (20)–(21) to eliminate the short-circuit current term $I_{f,a}$, the complex equation set $\mathbf{F_{ag}}(Z, \Delta V)$ is derived:

$$\mathbf{F_{ag}}(Z, \Delta V) = \begin{bmatrix} \dfrac{\Delta V_{i,m}}{\Delta V_{j,m}} - \dfrac{Z_{i_m f_a}}{Z_{j_m f_a}} \\ \dfrac{\Delta V_{i,m}}{\Delta V_{j,n}} - \dfrac{Z_{i_m f_a}}{Z_{j_n f_a}} \end{bmatrix} = \mathbf{O} \tag{22}$$

where m, n refer to different phases.

If only the voltage measurements taken from the faulted phase (ag) at both measurement points are considered, the reduced complex equation $F^{\mathrm{r}}_{\mathrm{ag}}(Z, \Delta V)$ is obtained:

$$F^{\mathrm{r}}_{\mathrm{ag}}(Z, \Delta V) = \frac{\Delta V_{i,a}}{\Delta V_{j,a}} - \frac{Z_{i_a f_a}}{Z_{j_a f_a}} = 0 \tag{23}$$

3) Analysis for Line-Line Short-Circuit Faults

For the case of a phase-a-to-phase-b (ab) fault, the boundary conditions are expressed by (17). Hence, (10)–(15) can be rewritten in the form of (24)–(25) when replacing $I_{f,b}$ by $-I_{f,a}$:

$$\Delta V_{i,k} = -(Z_{i_k f_a} - Z_{i_k f_b}) I_{f,a} \tag{24}$$

$$\Delta V_{j,k} = -(Z_{j_k f_a} - Z_{j_k f_b}) I_{f,a} \tag{25}$$

where $k = a, b, c$.

From (24)–(25), the complex equation set $\mathbf{F}_{\mathrm{ab}}(Z, \Delta V)$ is derived:

$$\mathbf{F_{ab}}(Z, \Delta V) = \begin{bmatrix} \dfrac{\Delta V_{i,m}}{\Delta V_{j,m}} - \dfrac{Z_{i_m f_a} - Z_{i_m f_b}}{Z_{j_m f_a} - Z_{j_m f_b}} \\ \dfrac{\Delta V_{i,m}}{\Delta V_{j,n}} - \dfrac{Z_{i_m f_a} - Z_{i_m f_b}}{Z_{j_n f_a} - Z_{j_n f_b}} \end{bmatrix} = \mathbf{O} \tag{26}$$

where m, n refer to different phases.

If only the voltage measurements taken from the faulted phases (ab) at both measurement points are considered, the reduced complex equation $\mathbf{F^r_{ab}}(Z, \Delta V)$ is obtained:

$$\mathbf{F^r_{ab}}(Z, \Delta V) = \begin{bmatrix} \dfrac{\Delta V_{i,a}}{\Delta V_{i,b}} - \dfrac{Z_{i_a f_a} - Z_{i_a f_b}}{Z_{i_b f_a} - Z_{i_b f_b}} \\ \dfrac{\Delta V_{j,a}}{\Delta V_{j,b}} - \dfrac{Z_{j_a f_a} - Z_{j_a f_b}}{Z_{j_b f_a} - Z_{j_b f_b}} \\ \dfrac{\Delta V_{i,a}}{\Delta V_{j,a}} - \dfrac{Z_{i_a f_a} - Z_{i_a f_b}}{Z_{j_a f_a} - Z_{j_a f_b}} \\ \dfrac{\Delta V_{i,a}}{\Delta V_{j,b}} - \dfrac{Z_{i_a f_a} - Z_{i_a f_b}}{Z_{j_b f_a} - Z_{j_b f_b}} \\ \dfrac{\Delta V_{i,b}}{\Delta V_{j,a}} - \dfrac{Z_{i_b f_a} - Z_{i_a f_b}}{Z_{j_a f_a} - Z_{j_a f_b}} \\ \dfrac{\Delta V_{i,b}}{\Delta V_{j,b}} - \dfrac{Z_{i_b f_a} - Z_{i_a f_b}}{Z_{j_b f_a} - Z_{j_b f_b}} \end{bmatrix} = \mathbf{O} \tag{27}$$

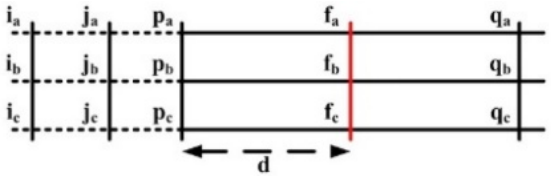

Fig. 2. Representation of a three-phase line segment.

4) Analysis for Double-Line-Ground Short-Circuit Faults

For the case of a phase-*a*-to-phase-*b*-to-ground (*abg*) fault, the boundary conditions are expressed by (18) where $I_{f,g}$ is the current through ground. Hence, (10)–(15) can be rewritten in the following form:

$$\Delta V_{i,k} = -Z_{i_k f_a} I_{f,a} - Z_{i_k f_b} I_{f,b} \tag{28}$$

$$\Delta V_{j,k} = -Z_{j_k f_a} I_{f,a} - Z_{j_k f_b} I_{f,b} \tag{29}$$

From (28)–(29), the following fault location equation set $\mathbf{F_{abg}}(\mathrm{Z}, \Delta V)$is derived:

$$\mathbf{F_{abg}}(Z,\Delta V) = \left[\frac{\Delta V_{i,k} Z_{j_m f_b} - \Delta V_{j,m} Z_{i_k f_b}}{\Delta V_{i,k} Z_{j_n f_b} - \Delta V_{j,n} Z_{i_k f_b}} - \frac{Z_{i_k f_b} Z_{j_m f_a} - Z_{i_k f_a} Z_{j_m f_b}}{Z_{i_k f_b} Z_{j_n f_a} - Z_{i_k f_a} Z_{j_n f_b}}\right] = \mathbf{O} \tag{30}$$

where *k* is one of the phases *a*, *b*, *c* and *m*, *n* represent a different combination between phases *a*, *b*, *c* for each *k* considered.

If only the voltage measurements taken from the faulted phases (*ab*) at both measurement points are considered, the reduced complex equation $\mathbf{F^r_{abg}}(Z,\Delta V)$ is obtained:

$$\mathbf{F^r_{abg}}(Z,\Delta V) = \begin{bmatrix}
\frac{\Delta V_{i,a} Z_{j_a f_b} - \Delta V_{j,a} Z_{ia f_b}}{\Delta V_{i,a} Z_{j_b f_b} - \Delta V_{j,b} Z_{i_a f_b}} - \frac{Z_{i_a f_b} Z_{j_a f_a} - Z_{i_a f_a} Z_{j_a f_b}}{Z_{i_a f_b} Z_{j_b f_a} - Z_{i_a f_a} Z_{j_b f_b}} \\
\frac{\Delta V_{i,a} Z_{j_b f_b} - \Delta V_{j,b} Z_{i_a f_b}}{\Delta V_{i,a} Z_{j_b f_b} - \Delta V_{j,b} Z_{i_a f_b}} - \frac{Z_{i_a f_b} Z_{j_b f_a} - Z_{i_a f_a} Z_{j_b f_b}}{Z_{i_a f_b} Z_{j_b f_a} - Z_{i_a f_a} Z_{j_b f_b}} \\
\frac{\Delta V_{i,a} Z_{j_a f_b} - \Delta V_{j,a} Z_{i_a f_b}}{\Delta V_{i,a} Z_{j_a f_b} - \Delta V_{j,a} Z_{i_a f_b}} - \frac{Z_{i_a f_b} Z_{j_a f_a} - Z_{i_a f_a} Z_{j_a f_b}}{Z_{i_a f_b} Z_{j_a f_a} - Z_{i_a f_a} Z_{j_a f_b}} \\
\frac{\Delta V_{i,a} Z_{j_b f_b} - \Delta V_{j,b} Z_{i_a f_b}}{\Delta V_{i,a} Z_{j_a f_b} - \Delta V_{j,a} Z_{i_a f_b}} - \frac{Z_{i_a f_b} Z_{j_b f_a} - Z_{i_a f_a} Z_{j_b f_b}}{Z_{i_a f_b} Z_{j_a f_a} - Z_{i_a f_a} Z_{j_a f_b}} \\
\frac{\Delta V_{i,b} Z_{j_a f_b} - \Delta V_{j,a} Z_{i_b f_b}}{\Delta V_{i,b} Z_{j_b f_b} - \Delta V_{j,b} Z_{i_b f_b}} - \frac{Z_{i_b f_b} Z_{j_a f_a} - Z_{i_b f_a} Z_{j_a f_b}}{Z_{i_b f_b} Z_{j_b f_a} - Z_{i_b f_a} Z_{j_b f_b}} \\
\frac{\Delta V_{i,b} Z_{j_b f_b} - \Delta V_{j,b} Z_{i_b f_b}}{\Delta V_{i,b} Z_{j_b f_b} - \Delta V_{j,b} Z_{i_b f_b}} - \frac{Z_{i_b f_b} Z_{j_b f_a} - Z_{i_b f_a} Z_{j_b f_b}}{Z_{i_b f_b} Z_{j_b f_a} - Z_{i_b f_a} Z_{j_b f_b}} \\
\frac{\Delta V_{i,b} Z_{j_a f_b} - \Delta V_{j,a} Z_{i_b f_b}}{\Delta V_{i,b} Z_{j_a f_b} - \Delta V_{j,a} Z_{i_b f_b}} - \frac{Z_{i_b f_b} Z_{j_a f_a} - Z_{i_b f_a} Z_{j_a f_b}}{Z_{i_b f_b} Z_{j_a f_a} - Z_{i_b f_a} Z_{j_a f_b}}
\end{bmatrix} = \mathbf{O} \tag{31}$$

5) Analysis for Three-Phase Short-Circuit Faults

For the case of a three-phase (*abc*) fault, the boundary conditions are expressed by (19). Hence, (10)–(15) can be rewritten in the following form when replacing $I_{f,c}$ by $-(I_{f,a}+I_{f,b})$:

$$\Delta V_{i,k} = (\underbrace{Z_{i_k f_c} - Z_{i_k f_a}}_{\Phi_k}) I_{f,a} + (\underbrace{Z_{i_k f_c} - Z_{i_k f_b}}_{X_k}) I_{f,b} \tag{32}$$

$$\Delta V_{j,k} = (\underbrace{Z_{j_k f_c} - Z_{j_k f_a}}_{\Psi_k}) I_{f,a} + (\underbrace{Z_{j_k f_c} - Z_{j_k f_b}}_{\Omega_k}) I_{f,b} \tag{33}$$

From (32)–(33), the following fault location equation set $\mathbf{F_{abc}}(Z,\Delta V)$ is derived:

$$\mathbf{F_{abc}}(Z,\Delta V) = \begin{bmatrix}
\frac{\Delta V_{i,k}\Omega_k - \Delta V_{j,k} X_k}{\Delta V_{i,m} X_n - \Delta V_{i,n} X_m} - \frac{\Phi_k \Omega_k - X_k \Psi_k}{X_n \Phi_m - X_m \Phi_n} \\
\frac{\Delta V_{i,k}\Omega_k - \Delta V_{j,k} X_k}{\Delta V_{j,n}\Omega_m - \Delta V_{j,m}\Omega_n} - \frac{\Phi_k \Omega_k - X_k \Psi_k}{\Psi_n \Omega_m - \Psi_m \Omega_n}
\end{bmatrix} = \mathbf{O} \tag{34}$$

where *k* is one of the phases *a*, *b*, *c* and *m*, *n* represent a different combination between phases *a*, *b*, *c* for each *k* considered.

Equation set (34) cannot be reduced since the voltage measurements taken from all the faulted phases (*abc*) of both measurement points are required.

C. Fault Position Estimation

Complex equation sets (23), (27), (31), and (34) are functions of the impedance terms and the phase voltage drops at the monitored buses. The desired distance *d* to fault position is encrypted into the impedance terms. Short-circuit phase current magnitudes are eliminated from this set. Moreover, although fault resistance is taken into account through its effect on the measured voltage drops, it is not explicitly included in the equations set. By separating the complex equation sets (23), (27), (31), and (34) into real and imaginary parts, the respective reduced algebraic equation sets are formed. Thereafter, the least squares method (LSM) is applied to estimate the distance *d* to the fault position.

The fault location algorithm holds equally for radial and DG-integrated distribution systems. Since multiple fault location solutions may be found, additional means such as fault passage indicators [16]–[18] can be installed in the system to assist in determining the faulty section.

III. Implementation Aspects

Voltage measurements can be taken from two arbitrary points of the distribution system of interest. Since there is always a voltage MD inside the main HV/MV substation (as shown in the indicative distribution system of Fig. 1), it is reasonable to take voltage measurements from this device. Then it is left to freely choose the second measurement point from a bus along the distribution feeder. A favorite second voltage measurement point is the terminal bus of a DG unit (if any DG unit is connected to the distribution network). This choice is justified since a DG unit for sure includes a voltage MD. In this way, the need of installing a voltage MD along the

feeder is eliminated. However, in case no DG unit is installed in the distribution system, any two measurement points could be arbitrarily chosen with the associated cost of the voltage MD. Hereafter, the measurement points will be arbitrarily selected to investigate the performance and robustness of the proposed method under various measurement combinations.

Moreover, the MDs at the two selected points should be able to provide synchronized voltage phasors from the collected voltage measurements. Fortunately, devices (e.g., numerical relays, micro phasor measurement units (μPMUs), smart meters, etc.) providing time-stamped voltage phasors with a common time reference like that determined by the global positioning system (GPS) are usually found in existing power systems. If not, there is a need to upgrade older equipment with new one. However, the replacement or installation of only two MDs with synchronized measurement capability costs relatively low nowadays.

Ultimately, the synchronized voltage phasors are gathered on a substation computer. The latter includes the FL (Fig. 1), which executes the fault location algorithms. This computer could be included in the distribution management system (DMS) of the distribution control center, also running several other functions, or it could be a machine dedicated for fault location applications. The entire fault location method application procedure is depicted in Fig. 3.

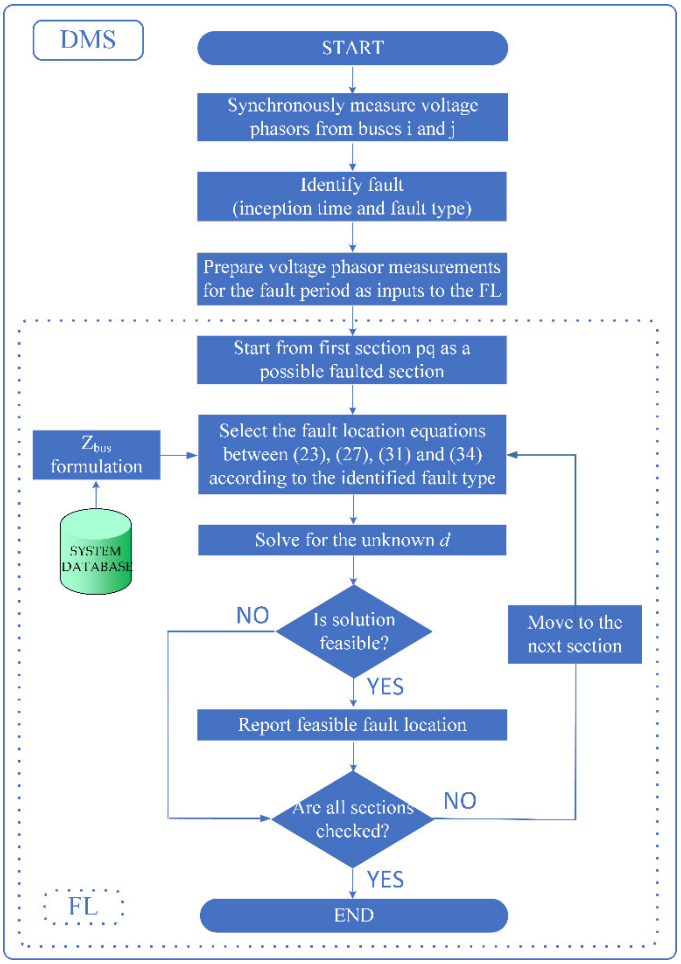

Fig. 3. Flowchart of the fault location method.

IV. Simulation Studies

A. Test System

The performance of the proposed algorithm is tested by conducting numerous simulation studies concerning the test distribution system of Fig. 4. This distribution system consists of three-phase, two-phase, and single-phase laterals and loads, whereas depending on the status of the circuit breakers (CB) at buses 17, 18, 19, and 20, a single-source or a multiple-source topology is alternatively assumed. The detailed data of this distribution system can be found in [4]. Note that the feeder shunt capacitances are ignored in the simulation model.

Both synchronous-machines-based (SMB) and inverter-interfaced DG units (in particular a PV unit) have been considered in the analysis, in order to demonstrate the performance of the proposed fault location algorithm with respect to fault current contribution from those DG units. The data of those units are given in the Appendix.

B. Procedure

EMTP-RV is used to simulate the short-circuit faults occurring in the test distribution system, whereas the proposed fault location algorithm is developed in MATLAB. The transient voltage waveforms measured at the recorded buses *i* and *j* are retrieved from the EMTP-RV simulations. Prior to the fault occurrence, that is during normal system state, the voltage at the monitored buses *i* and *j* is recorded with a sampling frequency equal to 1 kHz. When a fault is identified, the respective post-fault transient voltage waveforms at the monitored buses *i* and *j* are recorded with a sampling frequency equal to 20 kHz. The voltage samples are subsequently filtered through an anti-aliasing filter with cut-off frequency equal to 420 Hz. Finally, the discrete Fourier transform (DFT) is applied to reconstruct the corresponding voltage phasors, which are, then, sent from the MDs to the FL.

The FL runs the fault location algorithm which solves the proper equation set out of (23), (27), (31), (34) by utilizing the LSM of the MATLAB curve fitting tool. The estimation accuracy is calculated according to the equation below:

$$e(\%) = \frac{|d_a - d|}{l} \tag{35}$$

where d_a and d is the actual and estimated fault position respectively, and l is the total length of the main feeder.

The required bus impedance matrix $\mathbf{Z_{bus}}$ is systematically constructed in MATLAB according to the well-known three-phase circuit theory [19]. In fact, the $\mathbf{Z_{bus}}$ for each possible topology is predetermined and stored in a database.

C. Results

Three different system topologies are considered:

(i) a single-source topology (source at bus 1),

(ii) a double-source topology (source at bus 1 and 17),

(iii) a multi-source topology (source at bus 1,17,18,19,20).

All the common short-circuit types (i.e. SLG, LL, LLG, LLL) are simulated. For each specific fault type and line segment under investigation, the simulated fault position is varied along the segment in 10% length steps. Moreover, fault resistance from 0 up to 50 Ω is assumed.

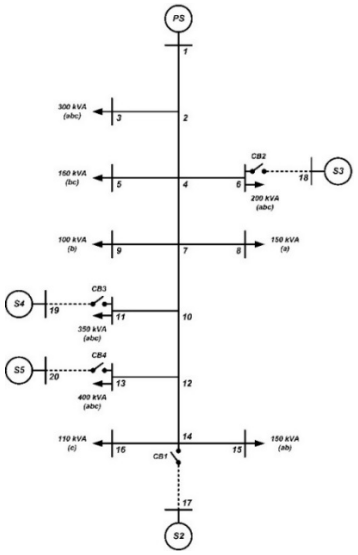

Fig. 4. Test distribution system.

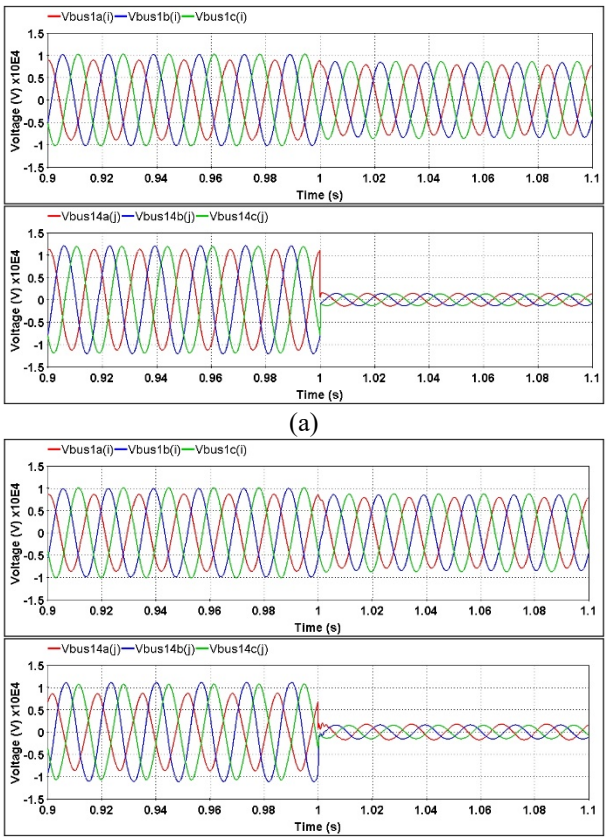

Fig. 5. Transient voltage waveform output. a) SMB unit, b) PV unit.

As an indicative example, Fig. 5 depicts the transient voltage waveforms recorded at buses 1 and 14 for a fault incidence at section 14-17 at time instant t = 1 s. Fig. 5a corresponds to the double-source topology with SMB units, whereas Fig. 5b corresponds to the multi-source topology with PV units. It should be noted that the DG unit output has been modified so as the total DG production be the same for both topologies.

Table I, II, III illustrate the results from the application of the proposed fault location algorithm assuming the topology (i), (ii), and (iii), respectively. The required voltage measurements are acquired from different pairs (i,j) of buses in order to illustrate the robustness of the method. The fault resistance magnitudes R_f assumed for each faulted phase as well as for the ground connection, if present, are also shown in Tables I, II, and III. The results show that a quite accurate fault position estimation is achieved. The latter is also validated by comparing the results of the proposed algorithm with that of the state-of-the-art method [4], which are shown in the eighth column of Tables I, II, and III.

TABLE I
RESULTS FOR SINGLE-SOURCE TOPOLOGY

Faulty Section	Fault Type	d_a (pu)	R_f (Ω)	e (%)			
				(i,j) *1,14*	(i,j) *6,13*	(i,j) *4,12*	[4]
1-2	ag	0.5	2.5,2.5(g)	0.002	0.003	0.003	0.020
	ab	0.5	5	0.036	0.025	0.026	0.022
	abg	0.5	2.5,2.5(g)	0.001	0.002	0.002	0.010
	abc	0.5	2.5	0.001	0.012	0.011	0.023
4-6	ag	0.7	5,10(g)	0.854	0.001	0.305	0.057
	ab	0.7	5	0.632	0.011	6.322	0.041
	abg	0.7	5,10(g)	0.310	0.004	1.743	0.043
	abc	0.7	10	3.011	0.001	4.780	0.055
7-10	ag	0.3	10,50(g)	0.001	0.001	0.001	0.097
	ab	0.3	5	0.074	0.026	0.026	0.052
	abg	0.3	10,50(g)	0.001	0.001	0.001	0.064
	abc	0.3	5	0.000	0.009	0.008	0.060
12-13	ag	0.8	5,20(g)	0.545	0.008	0.092	0.087
	ab	0.8	2.5	0.425	0.001	2.274	0.044
	abg	0.8	5,20(g)	0.150	0.008	0.750	0.064
	abc	0.8	5	1.053	0.004	2.551	0.093
12-14	ag	0.6	10,30(g)	0.012	0.093	0.091	0.092
	ab	0.6	5	0.068	6.990	6.991	0.061
	abg	0.6	10,30(g)	0.002	0.014	0.008	0.079
	abc	0.6	5	0.007	1.715	1.678	0.086
14-15	ag	0.4	5,10(g)	1.058	0.117	0.115	0.065
	ab	0.4	2.5	6.118	1.760	1.750	0.036
	abg	0.4	5,10(g)	0.210	0.117	0.115	0.053

TABLE II
RESULTS FOR DOUBLE-SOURCE TOPOLOGY

Faulty Section	Fault Type	d_a (pu)	R_f (Ω)	e (%)			
				(i,j) *1,14*	(i,j) *6,13*	(i,j) *4,12*	[4]
1-2	ag	0.5	2.5,2.5(g)	0.002	0.004	0.005	0.022
	ab	0.5	5	0.003	0.002	0.003	0.024
	abg	0.5	2.5,2.5(g)	0.002	0.003	0.003	0.050
	abc	0.5	2.5	0.001	0.004	0.005	0.023
4-6	ag	0.7	5,10(g)	0.356	0.002	0.237	0.056
	ab	0.7	5	1.720	0.004	5.178	0.031
	abg	0.7	5,10(g)	0.836	0.007	0.620	0.040
	abc	0.7	10	12.16	0.001	2.545	0.040
7-10	ag	0.3	10,50(g)	0.001	0.002	0.002	0.348
	ab	0.3	5	0.119	0.039	0.039	0.072
	abg	0.3	10,50(g)	0.002	0.002	0.002	0.099
	abc	0.3	5	0.001	0.005	0.005	0.086
12-13	ag	0.8	5,20(g)	0.270	0.006	0.131	0.081
	ab	0.8	2.5	0.489	0.008	2.264	0.051
	abg	0.8	5,20(g)	0.248	0.006	0.929	0.052
	abc	0.8	5	7.367	0.005	1.600	0.054
14-15	ag	0.4	5,10(g)	0.694	0.170	0.168	0.062
	ab	0.4	2.5	0.119	0.127	0.132	0.038
	abg	0.4	5,10(g)	0.088	0.063	0.119	0.049
14-17	ag	0.6	10,30(g)	0.001	0.004	0.004	0.675
	ab	0.6	5	0.041	0.079	0.079	0.184
	abg	0.6	10,30(g)	0.047	0.057	0.057	0.342
	abc	0.6	5	0.300	0.083	0.081	0.167

TABLE III
RESULTS FOR MULTI-SOURCE TOPOLOGY

Faulty Section	Fault Type	d_a (pu)	R_f (Ω)	e (%)			
				(*i*,*j*) *1,14*	(*i*,*j*) *6,13*	(*i*,*j*) *4,12*	[4]
1-2	ag	0.5	2.5,2.5(g)	0.013	0.002	0.002	0.020
	ab	0.5	5	0.008	0.006	X	0.021
	abg	0.5	2.5,2.5(g)	0.006	0.002	0.006	0.010
	abc	0.5	2.5	0.001	0.041	0.001	0.022
4-6	ag	0.7	5,10(g)	0.002	0.005	0.006	0.119
	ab	0.7	5	0.061	0.048	0.056	0.059
	abg	0.7	5,10(g)	0.002	0.008	0.001	0.080
	abc	0.7	10	0.330	0.001	0.032	0.093
7-10	ag	0.3	10,50(g)	0.002	0.005	0.003	0.265
	ab	0.3	5	0.110	0.046	0.033	0.072
	abg	0.3	10,50(g)	0.015	0.006	0.004	0.123
	abc	0.3	5	0.001	0.005	0.002	0.057
12-13	ag	0.8	5,20(g)	0.006	0.007	0.004	0.372
	ab	0.8	2.5	0.031	0.057	0.046	0.067
	abg	0.8	5,20(g)	0.030	0.003	0.013	0.108
	abc	0.8	5	0.097	0.001	0.050	0.086
14-15	ag	0.4	5,10(g)	0.895	0.365	0.342	0.057
	ab	0.4	2.5	0.119	0.127	0.132	0.037
	abg	0.4	5,10(g)	0.099	0.046	0.033	0.044
14-17	ag	0.6	10,30(g)	0.003	0.002	0.001	2.178
	ab	0.6	5	0.114	0.080	0.047	0.133
	abg	0.6	10,30(g)	0.029	0.040	0.026	0.240
	abc	0.6	5	0.376	0.003	0.012	0.102

D. Load Impedance Estimation

As discussed in Section II, the proposed fault location algorithm assumes that the $\mathbf{Z_{bus}}$ is known for a given distribution system topology. The construction of $\mathbf{Z_{bus}}$ supposes that the load of each system bus is also available. Although network data can be easily found, the load impedance at each bus can be hardly estimated. If there are no load data available at all, the load impedance can be estimated according to proper methods found in the literature [20],[21].

In this paper, the rated load impedances are assumed to be known. The results shown in Tables I, II, III are derived assuming the rated load values. In this subsection, a variation of the total load consumption which is measured at the substation is considered. Then, load impedances are recalculated (compensated) based on their rated values and the methodology described in [14]. Accordingly, an updated bus impedance matrix is calculated for each case. Table IV includes indicative results for 10%, 20% and 30% variation in total load for the single-source configuration. The measurement points at buses 1 and 14 are further considered. It is shown that fault position estimation accuracy is greatly improved in every case where load is compensated comparing to the case without load compensation.

E. Measurements Error Impact

The impact of measurement errors on the proposed algorithm accuracy is studied now. In these studies, errors of 1%, 2% and 3% in magnitude, and 3% error in magnitude together with 2° error in angle are introduced to the voltage phasors obtained at each measurement point. The worst-case scenarios have been considered, being those where the voltage measurements at each point have the maximum considered error with the opposite sign in the magnitudes. It can be seen from Tables V-VII corresponding to all the three system topologies (single-source, double-source, and multi-source, respectively) that the proposed algorithm is favorably not very sensitive to measurement errors for the indicative faults in the middle of sections 4-6, 10-11 and 11-14.

TABLE IV
RESULTS FOR LOAD VARIATION IN THE SINGLE-SOURCE CONFIGURATION

Faulty Section	Fault Type	d_a (pu)	R_f (Ω)	e (%)	
				Uncomp. (a) 10% (b) 20% (c) 30%	Compen. (a) 10% (b) 20% (c) 30%
1-2	ag	0.5	2.5	0.947	0.028
				1.776	0.046
				2.507	0.059
	ab	0.5	2.5	0.930	0.066
				1.386	0.140
				1.553	0.198
	abg	0.5	2.5	0.859	0.021
				1.606	0.034
				2.263	0.044
	abc	0.5	2.5	0.612	0.003
				1.128	0.006
				1.566	0.008
7-10	ag	0.3	10,50(g)	4.986	0.020
				9.356	0.111
				13.142	0.175
	ab	0.3	5	2.071	0.099
				5.566	0.189
				9.888	0.229
	abg	0.3	10,50(g)	1.022	0.025
				1.892	0.046
				2.638	0.061
	abc	0.3	5	0.479	0.020
				0.885	0.029
				1.228	0.035
12-14	ag	0.6	10,30(g)	7.601	0.092
				14.19	0.227
				19.91	0.323
	ab	0.6	5	13.74	0.285
				26.28	0.463
				37.78	0.603
	abg	0.6	10,30(g)	0.827	0.011
				1.551	0.025
				2.183	0.037
	abc	0.6	5	0.652	0.056
				1.189	0.089
				1.647	0.112

TABLE V
FAULT LOCATION FOR VOLTAGE MEASUREMENT ERRORS
(SINGLE-SOURCE TOPOLOGY)

Faulted section	**Fault type**	**Estimated error (e%) for measurement points 1-14**				
		0%	**1% in |V|**	**2% in |V|**	**3% in |V|**	**3% in |V| and 2° in angle**
4-6	ag	0.034	1.469	2.946	4.249	4.773
	ab	0.012	0.128	0.266	0.443	0.489
	abg	0.025	1.420	2.684	3.921	4.133
	abc	0.153	1.488	3.232	5.327	5.452
10-11	ag	0.022	1.842	3.617	5.349	5.773
	ab	0.003	1.617	3.198	4.747	5.282
	abg	0.004	2.692	5.023	7.047	7.762
	abc	0.092	1.117	2.198	3.247	3.282
11-14	ag	0.016	0.609	1.189	1.757	1.972
	ab	0.009	1.309	2.581	3.826	4.156
	abg	0.002	1.257	2.477	3.663	4.782
	abc	0.004	1.705	3.392	5.058	5.249

TABLE VI
FAULT LOCATION FOR VOLTAGE MEASUREMENT ERRORS
(DOUBLE-SOURCE TOPOLOGY)

Faulted section	Fault type	Estimated error (e%) for measurement points 6-13				
		0%	1% in |V|	2% in |V|	3% in |V|	3% in |V| and 2º in angle
4-6	ag	0.008	2.093	4.198	6.306	7.783
	ab	0.006	0.941	1.904	2.882	3.773
	abg	0.001	2.095	4.184	6.267	8.438
	abc	0.002	1.809	3.615	5.415	7.634
10-11	ag	0.011	0.178	0.350	0.536	0.572
	ab	0.008	0.229	0.444	0.661	0.729
	abg	0.011	0.369	0.714	1.053	2.552
	abc	0.035	2.112	4.874	7.207	8.984
11-14	ag	0.016	0.871	1.544	2.757	2.962
	ab	0.003	0.750	1.487	2.215	2.341
	abg	0.002	1.051	2.070	3.100	4.531
	abc	0.004	1.714	3.406	5.078	5.294

TABLE VII
FAULT LOCATION FOR VOLTAGE MEASUREMENT ERRORS
(MULTI-SOURCE TOPOLOGY)

Faulted section	Fault type	Estimated error (e%) for measurement points 4-12				
		0%	1% in |V|	2% in |V|	3% in |V|	3% in |V| and 2º in angle
4-6	ag	0.011	0.050	0.085	0.119	0.927
	ab	0.010	0.381	0.742	1.094	1.128
	abg	0.012	0.590	1.129	1.632	1.802
	abc	0.063	1.709	3.552	5.331	6.114
10-11	ag	0.140	1.904	4.120	6.211	6.976
	ab	0.320	2.306	4.442	9.211	10.32
	abg	0.135	2.242	5.074	9.907	9.984
	abc	0.059	2.532	5.114	10.21	10.84
11-14	ag	0.001	0.535	1.069	1.600	1.704
	ab	0.001	1.227	2.446	3.656	3.870
	abg	0.001	0.969	1.927	2.875	2.913
	abc	0.001	1.712	3.402	5.071	5.272

V. CONCLUSIONS

This paper addresses a fault location algorithm appropriate for unbalanced MV overhead distribution systems. The proposed algorithm utilizes only synchronized voltage measurements from two measurement points inside the distribution system, which makes it easily applicable and a low-cost solution for fault location application. The algorithm accurately estimates the fault position for any type of faults by applying fundamental bus-impedance-matrix-based fault analysis. Any type of DG units (i.e. SMB and/or IIDG units) can be dealt with by the algorithm as far as the appropriate model of DG unit is used. Simulation results show a good performance of the fault location algorithm under various pre-fault loading estimation conditions and measurement errors.

VI. APPENDIX

TABLE
MAIN DG PARAMETERS/CHARACTERISTICS

Synchronous-machine-based DG unit (Diesel Genset)	
Rated Power [kVA]	165
Frequency [Hz]	60
Rated Split Voltage L-L [kV]	0.48
Pole pairs	1
Xd / Xd'/ Xd'' [pu]	2.9/0.1/0.06
Xq / Xq" [pu]	1.740/0.071
Td'/ Td" / Tdo' / Ta [ms]	100/10/2865/15
Inverter-based DG unit (PV park)	
Rated Power [kVA]	500
Frequency [Hz]	60
Inverter Nominal Voltage L-L [kV]	0.575
Inverter Current limit (% Rated Current)	100
DC Input Voltage to the Inverter [kV]	1.264
Switching Frequency [Hz]	4500

VII. REFERENCES

[1] *A review of reliability of electric distribution system components*, EPRI white paper, 2001.

[2] R. A. F. Pereira, L. G.W. da Silva, M. Kezunovic, J. R. S. Mantovani, "Improved fault location on distribution feeders based on matching during fault voltage sags," *IEEE Trans. Power Del.*, vol. 24, pp. 852–862, Apr. 2009.

[3] J. Ren, S. S. Venkata, E. Sortomme, "An accurate synchrophasor based fault location method for emerging distribution systems," *IEEE Trans. Power Del.*, vol. 29, pp. 297–298, 2014.

[4] Y. Liao, "Generalized fault-location methods for overhead electric distribution systems," *IEEE Trans. Power Del.*, vol.26, pp. 53-64, Jan. 2011.

[5] M. Majidi, A. Arabali, M. Etezadi-Amoli, "Fault location in distribution networks by compressive sensing," *IEEE Trans. Power Del.*, vol. 30, pp. 1761–1769, Aug. 2015.

[6] F. C. L. Trindade, W. Freitas, "Low voltage zones to support fault location in distribution systems with smart meters," *IEEE Trans. Smart Grid*, ,vol. 8, pp. 2765–2774, 2017.

[7] K. Jia, B. Yang, X. Dong, T. Feng, T. Bi, D. Thomas, "Sparse voltage measurement-based fault location using intelligent electronic devices," *IEEE Trans. Smart Grid,* vol. 11, pp. 48–60, 2020.

[8] R. F. Buzo, H. M. Barradas, F. B. Leão, "A new method for fault location in distribution networks based on voltage sag measurements," *IEEE Trans. Power Del.*, in press.

[9] S. Lotfifard, M. Kezunovic, M. J. Mousavi, "Voltage sag data utilization for distribution fault location," *IEEE Trans. Power Del.*, vol. 26, pp. 1239–1246, Apr. 2011.

[10] F. C. L. Trindade, W. Freitas, J. C. M. Vieira, "Fault location in distribution systems based on smart feeder meters," *IEEE Trans. Power Del.*, vol. 29, pp. 251–260, Feb. 2014.

[11] Y. Dong, C. Zheng, M. Kezunovic, "Enhancing accuracy while reducing computation complexity for voltage-sag-based distribution fault location," *IEEE Trans. Power Del.*, vol. 29, pp. 251–260, Feb. 2014.

[12] R. Krishnathevar E. E. Ngu, "Generalized impedance-based fault location for distribution systems," *IEEE Trans. Power Del.*, vol. 27, pp. 449–451, Jan. 2012.

[13] M. Majidi, M. Etezadi-Amoli, M. S. Fadali, "A novel method for single and simultaneous fault location in distribution networks," *IEEE Trans. Power Systems*, vol. 30, pp. 3368–3376, Nov. 2015.

[14] S. S. Gururajapathy, H. Mokhlis, H. A. Illias, "Fault location and detection techniques in power distribution systems with distributed generation: A review," *Renew. Sustain. Energy Rev.*, vol. 74, pp. 949-958, 2017.

[15] N. Hussain, M. Nasir, J. C. Vasquez, J. M. Guerrero, "Recent developments and challenges on ac microgrids fault detection and protection systems–a review," *Energies*, vol. 13, 2149, 2020.

[16] K.Sun, Q.Chen, Z.Gao, "An automatic faulted line section location method for electric power distribution systems based on multisource information," *IEEE Trans.Power Del.*, vol.31, pp.1542-1551, Aug.2016.

[17] J. Teng, W. Huang, S. Luan, "Automatic and fast faulted line-section location method for distribution systems based on fault indicators," *IEEE Trans. Power Systems*, vol. 29, pp. 1653-1662, July 2014.

[18] P. S. Georgilakis, C. G. Arsoniadis, C. A. Apostolopoulos, V. C. Nikolaidis, "Optimal allocation of protection and control devices in smart distribution systems: Models, methods, and future research." *IET Smart Grid*, in press, https://doi.org/10.1049/stg2.12017.

[19] J. Grainger and W. Stevenson, *Power System Analysis*. New York: McGraw-Hill, 1994.

[20] S. J. Lee, M. S. Choi, S. H. Kang, B. G. Jin, D.S. Lee, B.S. Ahn, N. S. Yoon, H. Y. Kim, S.-B. Wee, "An intelligent and efficient fault location and diagnosis scheme for radial distribution systems," *IEEE Trans. Power Del.*, vol. 19, April 2004.

[21] R. Aggarwal, Y. Aslan, A. Johns, "New concept in fault location for overhead distribution systems using superimposed components," Proc. *IEE, Gen. Trans. Distr*., vol. 144, pp. 309–316, May 1997.